Mitigating COVID-19 Transmission in Schools With Digital Contact Tracing

Hao-Chen Sun, Xiao-Fan Liu, *Member, IEEE*, Zhan-Wei Du, Xiao-Ke Xu, *Member, IEEE*, and Ye Wu

***Abstract*— Precision mitigation of COVID-19 is in pressing need for postpandemic time with the absence of pharmaceutical interventions. In this study, the effectiveness and cost of digital contact tracing (DCT) technology-based on-campus mitigation strategy are studied through epidemic simulations using high-resolution empirical contact networks of teachers and students. Compared with traditional class, grade, and school closure strategies, the DCT-based strategy offers a practical yet much more efficient way of mitigating COVID-19 spreading in the crowded campus. Specifically, the strategy based on DCT can achieve the same level of disease control as rigid school suspensions but with significantly fewer students quarantined. We further explore the necessary conditions to ensure the effectiveness of DCT-based strategy and auxiliary strategies to enhance mitigation effectiveness and make the following recommendation: social distancing should be implemented along with DCT, the adoption rate of DCT devices should be assured, and swift virus tests should be carried out to discover asymptomatic infections and stop their subsequent transmissions. We also argue that primary schools have higher disease transmission risks than high schools and, thereby, should be alerted when considering reopenings.**

***Index Terms*— Asymptomatic infection, COVID-19, digital contract tracing, mitigation strategy, social distancing, susceptible-exposed-infectious-removed (SEIR).**

I. Introduction

THE COVID-19 pandemic has emerged into a global threat and was pseudonymously linked to more than 16 million and 600 thousand COVID-19-related cases and deaths as of July 2020 [1], albeit a mass of social distancing orders that have been enacted worldwide [2]. In the absence of pharmaceutical interventions, measures to reduce the overall burden of viral infection—including social distancing [3], case isolation [4], quarantine of susceptible [5], closure of public places [6], and increased availability of diagnostics—are paramount in planning for the months ahead [7]. Given the epidemiological disparity of strategies with the substantial economic and societal costs to sustain the virus transmission [8], there is a clear need for precision mitigation to alleviate the persistent burden of epidemics and prevent and respond effectively to future pandemics [9], [10].

Mass education is an indispensable foundation of modern society. Nevertheless, schools and universities, where teachers and students have long-term and intimate connections, are particularly risky areas for disease transmission [11]. To prevent campus outbreak, school suspension and closure of classes and grades are generally considered feasible approaches that can effectively reduce the number of infections [12]–[14]. However, school suspension or parts thereof can also result in a large number of students quarantined, either concentrated or at home, causing substantial socioeconomic costs and psychological problems [15]. Therefore, the critical question in effective retention lies in the selection of an effective mitigation strategy while inflicting a minimum cost to the society and economy [16].

Since large-scale human experiments with disease control measures are costly and risky to conduct, mathematical modeling offers a viable way to examine the impact of these measures with varying rates of controls [17]. Traditional transmission models are built upon mechanistic ones, such as the susceptible-infectious-removed (SIR) or susceptible-exposed-infectious-removed (SEIR) models [18]. However, the parameter settings of the models can vary among different diseases. Recently, animal experiments on cynomolgus macaques inoculated with the severe acute respiratory syndrome coronavirus 2 (SARS-CoV-2) have shown that the virus shedding can be presymptomatic and volatile [19]. Based on this finding, we propose an SEIR model with a variable infection rate that takes into account the frequent shift of SARS-CoV-2 from infections hence their transmissibility.

Except for the realistic transmission model, realistic assumptions, such as the accurate demographic data of a specific scenario, are also the prerequisite of epidemic modeling with validating results [20]. The realistic demographic

Manuscript received January 25, 2021; revised March 26, 2021; accepted April 11, 2021. This work was supported in part by the National Natural Science Foundation of China under Grant 61773091, Grant 11875005, Grant 61976025, and Grant 11975025; in part by the Liaoning Revitalization Talents Program under Grant XLYC1807106; in part by the Natural Science Foundation of Liaoning Province, China under Grant 2020-MZLH-22; and in part by the Major Project of the National Social Science Fund of China under Grant 19ZDA324. *(Hao-Chen Sun and Xiao-Fan Liu are co-first authors.) (Corresponding authors: Xiao-Ke Xu; Ye Wu.)*

Hao-Chen Sun and Xiao-Ke Xu are with the College of Information and Communication Engineering, Dalian Minzu University, Dalian 116600, China (e-mail: 2332697351@qq.com; xuxiaoke@foxmail.com).

Xiao-Fan Liu is with the Web Mining Laboratory, Department of Media and Communication, City University of Hong Kong, Hong Kong (e-mail: xf.liu@cityu.edu.hk).

Zhan-Wei Du is with the WHO Collaborating Centre for Infectious Disease Epidemiology and Control, School of Public Health, LKS Faculty of Medicine, The University of Hong Kong, Hong Kong, and also with the Laboratory of Data Discovery for Health, Hong Kong Science and Technology Park, Hong Kong (e-mail: duzhanwei0@gmail.com).

Ye Wu is with the Computational Communication Research Center, Beijing Normal University, Zhuhai 519087, China, and also with the School of Journalism and Communication, Beijing Normal University, Beijing 100875, China (e-mail: yewu@bnu.edu.cn).

Digital Object Identifier 10.1109/TCSS.2021.3073109

assumption mainly relies on high-resolution human interaction data. Common ways of acquiring such data include radio frequency identification devices (RFID) tracing [21], GPS tracing [22], Wi-Fi hotspot sharing [23], and other proximity traces, such as student card presences [24], [25]. In this study, we use two empirical data sets of wearable RFID devices' proximity collected from a primary school [26] and high school [21], [27], to construct temporal networks of campus interactions. The spatial proximity of two RFID devices resembles a close contact scenario that most probably facilitates the COVID-19 transmission.

Digital contact tracing (DCT) is a new and valuable technology based on mobile applications to understand the routes and timings of transmission [28]. Tracing devices, e.g., mobile phones or RFID, can log their mobility or close contacts with other devices so that wearers can monitor their virus exposure in a timely fashion [29]. Many governments have used smartphone contact tracing apps to automate the difficult task of tracing all recent contacts of newly identified infected individuals [30]. Researchers have verified the effectiveness of DCT by constructing a contact network of 115 students at a certain university [31] or setting a model of individual-level transmission based on 40 162 participants [32]. At present, there are few DCT studies on the cluster environment, and considering the easiness of technology adoption, this method can potentially provide a cost-effective solution to early detection, case isolation, and outbreak prevention of COVID-19 in certain environments where the population density is high, such as on campus.

In this study, we examine the effectiveness and cost of several mitigation strategies on campus, including the ones that utilize the newly proposed DCT technology. The effectiveness is measured by the number of infected students and the cost of the quarantined students. Compared with traditional suspension and closure methods, the DCT-based quarantine strategy can control disease-spreading much more efficiently. Necessary conditions for ensuring the DCT-based strategy's effectiveness and possible auxiliary strategies that provide further enhancement are also explored, including the social distancing strategy, the DCT device adoption rate, the influence of community infections, and the asymptomatic infections in the population. The results obtained from this study are expected to significantly impact the making of school policies in the post-pandemic era.

The rest of this article is organized as follows. Section II describes the student and teacher contact data sets, constructs temporal contact networks, proposes the COVID-19 variable infection model, and demonstrates disease spreading in the real-life network without mitigation measures. Section III discusses several mitigation strategies, including the closure of classes and grades, as well as one that is based on DCT, and their potential interventions to our proposed model. Section IV demonstrates the effectiveness and cost of different mitigation strategies, considering influences from further external factors, such as the proportion of asymptotic infections, the influences of social distancing and community infections, and the DCT device adoption rate in schools. Section V concludes this study.

II. Data Description and Epidemic Models

A. High-Resolution Empirical Contact Networks

To reconstruct the contact patterns of students and teachers within schools, we use two empirically collected real-time high-resolution on-campus contact data sets provided by SocioPatterns Collaboration [21], [26], [27]. One of the data sets contains the contacts among 232 primary school pupils and ten teachers, covering two days of school activities. Another data set contains the contacts among 329 high school students, covering five days of school activities. Students and teachers wear RFID sensors that activate every 20 s. Surrounding sensors within certain proximity are detected and logged. The teachers and students can make contact with each other in various scenarios, such as in-class teaching and learning, outdoor exercises, and dining. Thus, each contact network $G(i)$ is a temporal network $G(T) = \{G(1), G(2), \ldots, G(i), \ldots\}$, in which the students and teachers are the nodes and two nodes are connected by an undirected edge in $G(i)$ if proximity is logged by either sensor at the ith sensor activation.

Because the recorded school activities only span two days and five days in the two data sets, the data have to be expanded for extended time simulation. Considering that most schools have regular and periodic activities and open five days a week, the following expansions are made to the sample data sets, which also agrees with the previous literature [13]. For the primary school data, the two days of school activities are used interlaced in school days. During Saturdays and Sundays, teachers and students are considered with no contact. For the high school data, the five-day activities are used for each Monday-to-Fridays. Teachers and students are also considered with no contact in the schools during weekends. Considering that the teachers and students can also be exposed to hazardous environments after school on workdays and weekends, we study the community infections into the model and their influence on the DCT-based quarantine strategy in Section IV-D.

B. Epidemic Model With Variable Infection Rate

Compartmental models are commonly used to describe the progress of infectious diseases in a population. In an SIR model, an individual can be in each of the three states: Susceptible (S), Infectious (I), and Removed (R). An individual starts in a susceptible state and has a probability of transferring to the infectious state, in which they show symptoms and are infectious. After an infected individual recovers from or die of the disease, they enter the removed state, are assumed permanent immunity and, thereby, can no longer be infected again. The SEIR model builds upon the SIR model but adds an Exposed (E) state to incorporate the incubation period in which the individual has been infected but has not demonstrated any symptom and is not infectious yet. SIR has been used to model the spreading of many infectious diseases, such as SARS [33] and SEIR for the seasonal influenza [18].

In typical SIR and SEIR models, whenever a susceptible individual is in contact with an infectious individual, its probability p of becoming infected continually increases with the exposure time Δt at a constant rate β_{const}, i.e., $p = \beta_{\text{const}} \Delta t$,

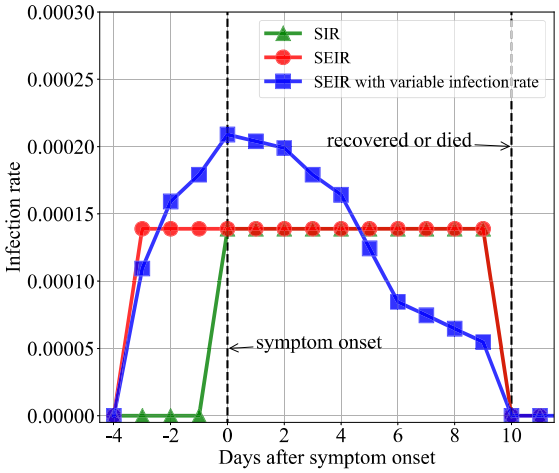

Fig. 1. Constant and variable infection rate models. The accumulative transmissibilities of the variable SEIR and constant (SEIR) infection rate models, i.e., the areas under the red and blue lines, are the same.

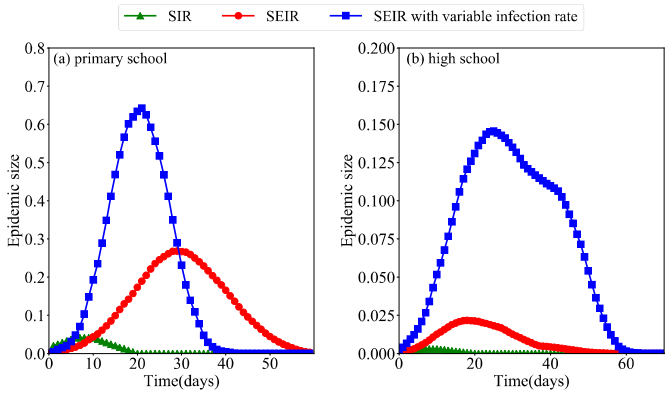

Fig. 2. Averaged epidemic spreading curves in (a) primary school and (b) high school using three different infection rate models. Day 0 represents the Monday of the first week.

as shown in Fig. 1. If $\beta_{\text{const}}\Delta t > 1$, the susceptible must be infected. Especially, a constant infection rate assumes that the virus shedding volume during the infectious period is constant. However, this assumption is not true for SARS-CoV-2.

Animal experiments on cynomolgus macaques inoculated with SARS-CoV-2 have shown that the transmissibility of COVID-19 varies with time. The virus shedding volume from macaques gradually increases from the first day after infection, peaks, and gradually decreases until recovery or death [19]. Based on the empirical virus shedding volumes in each day $E(t)$, we characterize the transmissibility of COVID-19 with a variable infection rate in Fig. 1.

Three assumptions are made in the variable infection rate model. First, the infection rate is proportional to logged virus shedding volume, i.e., $\beta(t) \sim \log E(t)$ [34], [35]. Note that, since the shedding of SARS-CoV-2 starts from day one, our model is effectively an SEIR model. Second, the average cure time of COVID-19 is 14 days, i.e., an incubation period of four days median [36] and a recovery period with ten days on average [37]. That is to say, different from the traditional SIR model where an infected individual shows symptoms once they enter the Infectious state, our model assumes that the infected individuals can transmit the virus for four days undetected. Third, the accumulated transmissibilities of the SEIR models with variable and constant infection rates are the same, i.e., $\sum_{t=1}^{14} \beta(t) = \beta_{\text{const}} \times 14$.

C. Transmissibility of Different Infection Models

We compare the transmissibility of the three infection rate models using Monte Carlo simulations. The simulations were programed with Python programming language and run on six-core CPUs, 32-GB memory space, and Windows 10 operating system. Each of the simulations runs 5000 times to encounter the randomness in the epidemic spreading process.

Relevant studies have shown that the R_0 value of COVID-19 is between 2.2 and 5.7 [38], [39]. The purpose of this study is to verify the effectiveness of DCT in primary and high schools. Considering the significant difference in the density of contact between primary and high schools, we set different R_0 values for primary and high schools respectively. Based on R_0, we can set the suitable infection rates for primary and high schools. The infection rates in different models are set with the assumption of $\beta_{\text{const}} = 1.38 \times 10^{-4}$ s^{-1}, i.e., a 120-min accumulated contact time can guarantee an infection, in the primary school, and $\beta_{\text{const}} = 2.76 \times 10^{-4}$ s^{-1} in the high school. Whenever a symptom onset is detected, only the symptomatic infection is removed from the model, and no other mitigation measures are taken.

As shown in Fig. 2, our model significantly advances the epidemic peaks for several days compared to the SEIR model and enlarges the epidemic sizes when one happens. The SIR model, on the contrary, generates very few epidemics comparatively. The reason for such strong transmissibility of our proposed epidemic model is that infected individuals can be infectious for four days before being discovered than only one day in the SIR model. Meanwhile, the virus shedding volume surges on and before the symptom onset date. This result highlights the necessity of a swift mitigation measure for epidemic prevention to COVID-19 on campus.

III. Mitigation Strategies

This study aims to examine the effectiveness and cost of the DCT-based mitigation strategy for COVID-19 spreading on campus. The effectiveness of a strategy is measured by the number of infections in the school. The cost is measured by the number of teachers and students isolated or quarantined. Traditional on-campus mitigation strategies, such as the temporary closure of classes, are employed as comparative measures.

A. Traditional Mitigation Strategies

School suspension and closure of grades and classes are generally considered feasible control measures for epidemic spreading on campus but vary in their effectiveness and cost. Effective distance, which has been proven a feasible measure for evaluating the possibility of disease transmission between

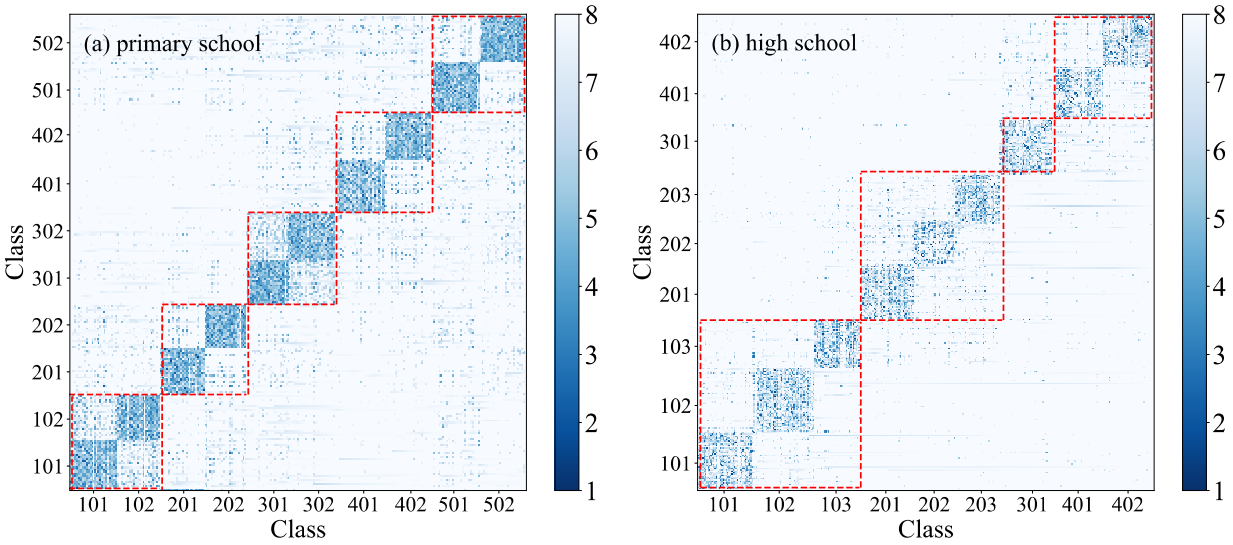

Fig. 3. Effective distance matrixes of (a) primary school and (b) high school. The labels on the axes indicate the grade and class to which the students belong, e.g., 201 means class 1 of grade 2.

two individuals, especially for infectious respiratory viruses, such as H1N1 and SARS [40], can help comprehend the rationale behind these traditional mitigation strategies. The effective distance d_{mn} between two individuals m and n in a contact network is defined as

$$d_{mn} = 1 - \log P_{mn} \tag{1}$$

in which the contact probability is given as

$$P_{mn} = \frac{I_{mn}}{G_m} \tag{2}$$

where I_{mn} represents the number of contact between m and n, and G_m represents the total number of contacts of m. d_{mn} ranges from 1 to infinity. A short effective distance can accelerate virus spreading, while a large effective distance will hinder the spreading of infectious diseases.

The effective distance matrices of the primary and high school teachers and students are shown in Fig. 3. The primary school is composed of five grades, and each grade includes two classes, thus a total of ten classes. The high school is composed of four grades and a total of nine classes. In Fig. 3, the darker the blue, the smaller the effective distance, and the more easily the virus spreads. It can be seen that students in the same class form a dark blue grid, and the effective distances are mostly shorter than 4, which means that the virus can more easily spread within a class. A red box represents a grade. In primary school, the contact is slightly closer in grades 1 and 3 and slightly sparser in grades 2, 4, and 5. In high school, although there are fewer contacts between classes, the connections with the same grade are still denser than between grades. That is to say, the virus can spread between classes in the same grade. Therefore, commonly used mitigation strategies for infectious diseases on campus with ascending rigidity and effectiveness involve the following.

1) *Case Isolation:* Whenever a student shows symptoms, they are isolated from the rest of the students for some time.
2) *Class Closure:* Whenever the number of symptomatic individuals in a class reaches a fixed threshold, the class is closed for some time;
3) *Grade Closure:* Whenever the number of symptomatic individuals in a grade reaches a fixed threshold, the grade is closed for some time;
4) *School Closure:* Whenever the number of symptomatic individuals in the school reaches a fixed threshold, the whole school is closed for some time.

Two key parameters control the intensity of a mitigation measure: the strategy trigger threshold, e.g., the number of symptomatic individuals detected, and the duration of the isolation or closure. This study considers the trigger threshold to be 1 and the isolation duration to be 14 days. For example, whenever a symptom onset is detected in a class, all the classmates must be quarantined for 14 days under the class closure strategy. Classes, grades, and schools can be closed again after reopening.

B. Quarantine Strategy Based on Digital Contact Tracing

The traditional class and grade closure strategies, in which all the students within the same classes or grades are quarantined because of their assumptive close contact with the symptomatic individual, can be an overreaction: those who are forced to quarantine but had no direct exposure to the disease do not contribute to the epidemic mitigation yet lose their opportunity of normal education. In contrast, the DCT technology can precisely identify the most probable disease exposures.

Considering that any logged proximity between two individuals using DCT is a close contact regardless of duration, and any nth order contacts of the initial infection can be

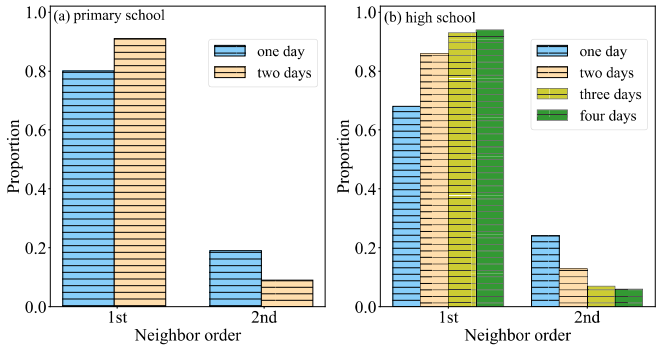

Fig. 4. Disease's transmission range, i.e., furthest order of initial infection's neighbor that it reaches, in (a) primary school and (b) high school.

traced back and send to quarantine, covering all their subsequent infections. DCT-based strategy's mitigation effectiveness depends on the selection of n. Given a single symptomatic infection in our model, the probability of their transmission range, i.e., the furthest order of neighbor that the disease reaches, is shown in Fig. 4. Since the incubation period of the patient is four days, we consider the transmission range of the patient within four days. The primary school data set only includes the two days of school activities, so the result of four days is the same as that of two days, and we only show the transmission range of two days in the primary school.

In most cases, the disease only transmits for one generation and seldom over two generations. Therefore, we propose a mitigation strategy based on DCT that, whenever an infection is discovered, they and only their first-order close contacts in four days before the infections, who are discovered, should be quarantined. The quarantine time is also set to be 14 days, as same as in the traditional strategies. If teachers and students do not show symptoms after the quarantine, they return to the school.

IV. Experimental Results

This section presents the effectiveness and cost of different mitigation strategies drawn from Monte Carlo simulations. The simulations were programed with Python programming language and run on six-core CPUs, 32-GB memory space, and Windows 10 operating system. Each of the simulations runs 5000 times to encounter the randomness in the epidemic spreading process.

We used SEIR with variable infection rates for simulation. The simulations are run with three assumptions. First, only one infection is randomly placed at the beginning of each simulation. Second, if an individual is infectious, they can transmit the disease for the whole day. The contact duration between two individuals is accumulated by all their discrete contact periods on each day. Third, teachers and students are checked for symptoms at the end of each day. Only symptomatic individuals can be detected. Individuals in the incubation period or asymptomatic individuals cannot.

TABLE I

Epidemic Probabilities P_e and Medians of Numbers of Quarantined Individuals N_q Under Different Mitigation Strategies

Place	Primary school		High school	
Mitigation measures	P_e	N_q	P_e	N_q
Case isolation	94.1%	224	71.2%	86
Class closure	36.6%	46	2.4%	67
Grade closure	21.8%	90	0.9%	111
School closure	2.8%	242	0.0%	329
DCT-based quarantine	**4.4%**	**96**	**0.0%**	**49**

TABLE II

Precision and Recall of Different Mitigation Strategies

Place	Primary school		High school	
Mitigation measures	Precision	Recall	Precision	Recall
Case isolation	100%	18%	100%	30%
Class closure	30%	64%	14%	88%
Grade closure	20%	75%	6.0%	91%
School closure	4.0%	100%	1.7%	100%
DCT-based quarantine	**13%**	**91%**	**17%**	**92%**

A. Effectiveness and Cost of Mitigation Strategies

The effectiveness is measured by the number of infections, and the cost by the man time of quarantined individuals. We consider an epidemic being formed on campus whenever more than 10% of the teachers and students are infected. Table I shows the epidemic probabilities P_e, i.e., the proportion of simulations that lead to epidemics, under each mitigation strategy and the median numbers N_q of teachers and students quarantined in both schools.

As the level of closure order escalates, the probability of an epidemic decreases. With only case isolation, i.e., no mitigation measure is taken, more than 94.1% and 71.2% simulations lead to epidemics in the primary and high schools, respectively. The DCT-based quarantine strategy can achieve the same levels of control as school suspension but with significantly smaller numbers of quarantined individuals.

Table II shows the precision, i.e., the proportion of total infected individuals to total quarantined individuals under each measure, and the recall, i.e., the proportion of total infected individuals in quarantine to total infected individuals. We calculate precision and recall when implementing measures for the first time. Although the precision of case isolation is 100%, the recalls in primary school and high school are only 18% and 30%. After the first isolation, 82% or 70% of cases still spread the virus in schools. In primary school, the precision of DCT is lower than class and grade closures because the students have more first-order neighbors. The situation in high school is the opposite. In both schools, the precision of the DCT measure is higher than school closure, and the recall is higher than class and grade closures, with a value of over 90%. Considering that the disease is most transmissible between close contacts,

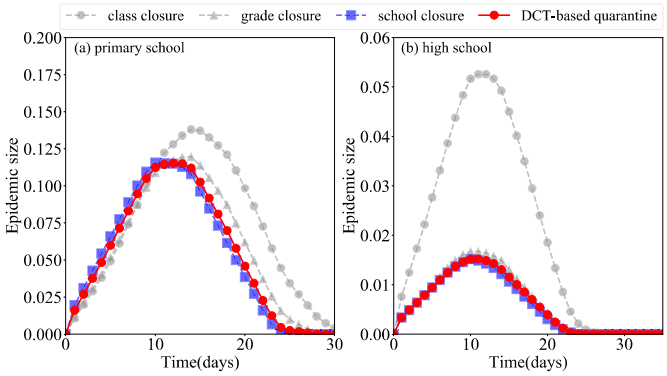

Fig. 5. Averaged epidemic spreading curves in (a) primary school and (b) high school under different mitigation strategies.

DCT can precisely identify the most probable individuals rather than brutally shutting down the whole school. However, the DCT-based strategy's effectiveness is still lower than school suspension, as there is still a certain probability that the disease can spread to the initial infections' second-order contacts with four days of transmission.

Mitigation strategies can not only decrease the epidemic probability but also lowers the epidemic size when one happens, although with variable effectiveness. We define epidemic size as the proportion of infected teachers and students in a school when an epidemic occurs. Fig. 5 shows the averaged epidemic curves under different mitigation strategies. In primary school and high schools, the peak values of case isolation are 0.6 and 0.14, respectively. The results are significantly different from the other three measures. To better illustrate the differences between the other three measures, we did not add this curve in Fig. 5. In both primary and high schools, class closure provides the lowest mitigation capability. The DCT-based quarantine can achieve similar results to school closure, which is the most rigid mitigation action and achieves the most substantial epidemic size reduction in both the primary and high schools.

B. Influence of Social Distancing

The epidemic probability and size in primary school are notably higher and larger than in high school. The reason is that the density (i.e., the average number of individuals' contacts) and the intensity (i.e., the duration of close contacts among teachers and students) of the primary school contact network are different from those in the high school contact network. Fig. 6 shows the distributions of first- and second-order neighbors in the primary and high schools. In primary school, almost every pair of pupils can be connected within two hops, while, in high school, students are more sparsely connected.

If one can reduce the density and intensity of a contact network, naturally, the epidemic can be better controlled. Social distancing policies, e.g., calling off social gathering events and wearing masks, are feasible yet easy-to-implement nonpharmaceutical measures to lower the network density and reduce the contact intensity. Here, we evaluate the impact of additional social distancing policies enforced alongside the DCT-based mitigation strategy.

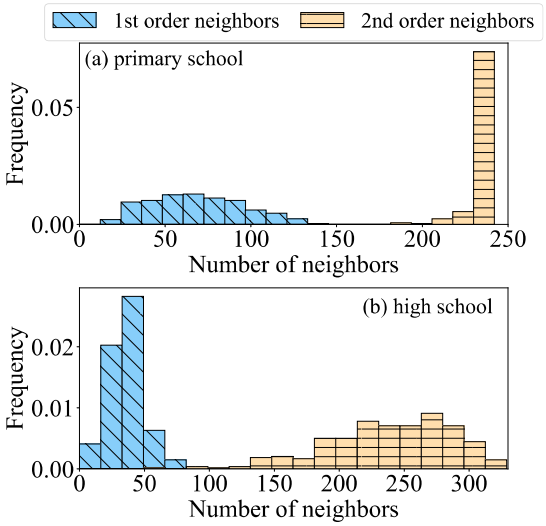

Fig. 6. Distributions of individuals' numbers of first- and second-order neighbors in both (a) primary school and (b) high school.

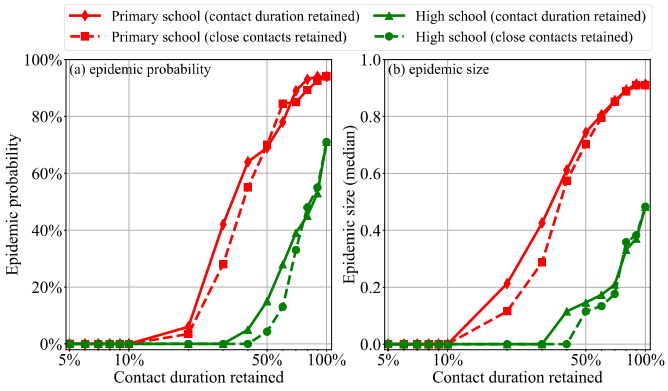

Fig. 7. Influence of social distancing on epidemic risks in both primary and high schools. (a) Epidemic probability and (b) epidemic size both increase monotonically with the proportion of contact duration retained.

Edges in the contact networks are randomly removed to mimic the scenario of calling off social gathering events. The contact duration, i.e., the weight of the contact networks, is proportionally reduced to mimic the scenarios, such as reduced social activities. The influence of social distancing policies on the epidemic probability and size in both schools is shown in Fig. 7. The epidemic size is the median of the cumulative number of cases in the simulations where the epidemic can occur. That is, the number of infected individuals is greater than 10% of the total number of students. The epidemic probability and sizes both decrease monotonically with the proportions of contacts removed and contact duration reduced. Epidemics can even be entirely prevented if social distancing is reduced to 10% of the normal level. Therefore, imposing social distancing policies can enhance the effectiveness of a DCT-based quarantine strategy.

C. Influence of DCT Device Adoption Rate

To implement the DCT-based strategy, teachers and students have to wear RFID devices or install specific applications

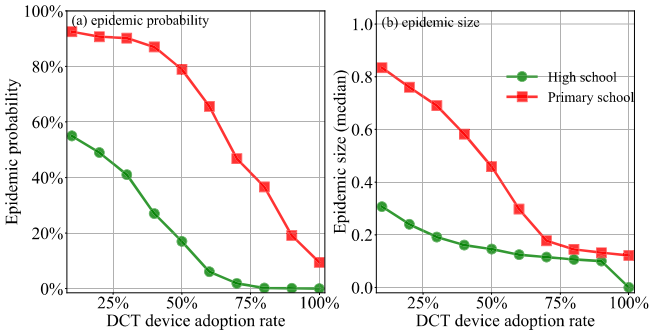

Fig. 8. Influence of DCT device adoption rate on (a) epidemic probabilities and (b) epidemic sizes.

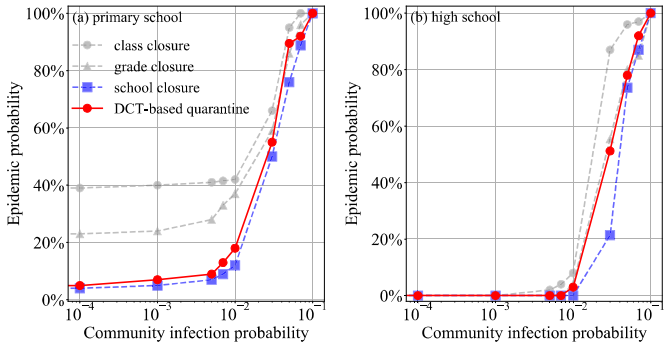

Fig. 9. Influence of community infection probability to the mitigation effectiveness in (a) primary school and (b) high school.

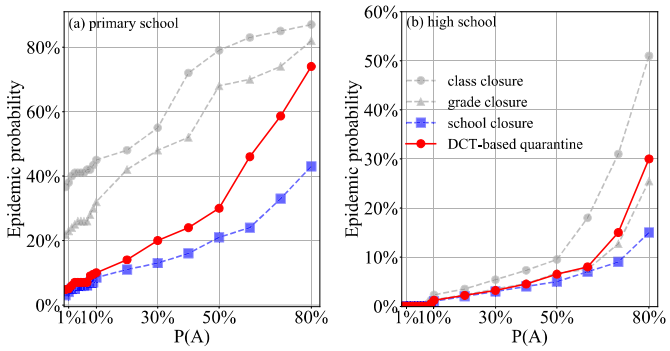

Fig. 10. Influence of asymptomatic infections to the mitigation effectiveness in (a) primary school and (b) high school.

on their mobile phones. Although this method is proven to mitigate epidemics, it could, nonetheless, raise privacy concerns. Therefore, it is natural to assume that some teachers or students will not adopt this tracing technology. In this section, we analyze the impact of the adoption rate on this mitigation action.

Fig. 8 shows the changes in epidemic probability and size with the DCT device adoption rate. The higher the adoption rate, the less probable that an epidemic forms on campus. Note that the epidemic probability sharply decreases when the adoption rate is greater than 50% in primary school and 25% in high school, respectively. The epidemic size also decreases with the adoption rate, from close to 0.8, with less than 25% adoption rate to around 0 with 100% adoption rate, in both the primary and high schools. In light of these results, we recommend that, if schools adopt a DCT-based strategy for epidemic control, it must be implemented with continuous monitoring to ensure its effectiveness.

D. Influence of Community Infections

In the previous scenarios, we assume that the only infection source is the one incorporated into the model on day 0. However, considering that the teachers and students can also be exposed to hazardous environments after school, we introduce community infections into the model.

Specifically, an individual in a susceptible state has a probability of being infected at home or other social events. Depending on the community infection rate, variable numbers of infections can be introduced into our model each day. Fig. 9 shows the epidemic probability in both the primary and high schools with variable community infection probabilities. When the community infection probability is larger than 0.01, i.e., approximately one infection can be introduced each day or two, the epidemic probability sharply increases. However, the DCT-based quarantine strategy still outperforms the closure of classes and grades and close to school suspension.

In the light that infections introduced externally can severely jeopardize the mitigation effectiveness of any strategy, schools should be always be alerted and prevent any imported infections from outside of campus.

E. Influence of Asymptomatic Infections

Asymptomatic infections are infections that do not show any symptoms and, therefore, cannot be discovered with naked eyes without nucleic acid tests. Therefore, the virus transmission period of the asymptomatic infections can be 14 days rather than four days for symptomatic infections for COVID-19. In this analysis, we tune the proportion of asymptomatic infections in our model and analyze their impact on the effectiveness of mitigation strategies. Note that the disease transmissibilities of symptomatic individuals and asymptomatic individuals are considered the same.

An individual can be set as asymptomatic with probability $P(A)$ and symptomatic with probability $1 - P(A)$. The epidemic probabilities under all mitigation strategies with different asymptomatic probabilities $P(A)$ are shown in Fig. 10. The result of primary school shows that the epidemic probability can increases with $P(A)$ almost linearly. In high school, the epidemic probability increases with $P(A)$ only when $P(A)$ is greater than 10%. The reason is that there is less contact between high school students. Even if there are asymptomatic patients, the probability that the patients can infect others is lower, and the number of asymptomatic patients is relatively small when $P(A)$ is less than 10%.

When $P(A)$ is greater than 10%, the epidemic probability of the two schools can increase as $P(A)$ increases, and when $P(A)$ is high, the virus can spread to the second-order neighbors, so the effect of first-order DCT is relatively weak. It should be noted that the prevention and control effect of grade closure is weak in primary school but effective in high school. When $P(A)$ is greater than 60%, the prevention and control effect of grade closure is even better than DCT. This is because there is almost no contact between students of

different grades in high school, and the virus is difficult to spread to other grades. Therefore, even if there are asymptomatic patients, closed grades have a strong effect in high school.

In summary, considering that $P(A)$ of COVID-19 can range from 10% to 80% [41], [42], epidemics can easily happen in the presence of asymptomatic infections. Therefore, before the outbreak of the epidemic, students should be encouraged to wear masks or maintain social distancing to reduce the spread of the virus. Whenever a case is detected, strict virus testing methods, such as nucleic acid or serum testing, are encouraged to avoid epidemics. In the implementation of DCT, second-order neighbor tracking can also be considered.

V. Conclusion and Discussion

DCT with wearable hardware is a new and effective epidemic mitigation strategy that could be used to fight against highly infectious diseases, such as COVID-19. In this study, we proposed to examine its effectiveness and cost, quantified by the numbers of infections and quarantined individuals, respectively, in controlling disease spreading on campus. Two empirical high-resolution on-campus interpersonal close contact data sets and a modified SEIR model with a variable infection rate setting are employed to simulate epidemics. Compared to traditional mitigation strategies, such as the closure of classes, grades, and the whole school, the DCT quarantine strategy can achieve a similar effect as more rigid strategies but with a much smaller cost.

Several factors can strongly affect the mitigation effectiveness of the DCT-based strategy. First when the probability of asymptomatic is high, the prevention and control effects of various strategies will be weakened as they can transmit the disease for an extended period than symptomatic infections, who are isolated as soon as they show any symptom. Second, community-introduced infections can jeopardize the efforts made by any mitigation strategy. Third, the adoption rate of teachers and students profoundly affects the effectiveness of the DCT-based strategy. Fourth, social distancing can help with the mitigation strategy and further increase its effectiveness.

In light of the above results, we make the following recommendations to the on-campus mitigation of COVID-19. First, a DCT-based strategy is encouraged in schools. Second, the strategy's adoption rate must be monitored and assured continuously. Third, whenever an infection is detected on campus, rigid virus testings must be carried out to a larger extent of the population for asymptomatic or community-introduced case discovery. Fourth, social distancing measures must be placed in schools to minimize the probability of disease spreading.

Note that the density of the primary school empirical contact network is much higher than that in the high school. Although the contact data are collected from two individual schools in a particular period, we argue that this phenomenon can be universal, as pupils in primary schools are more physical activity-intensive (i.e., having more physical contacts) than students in the high schools, who are in contrast more academic activity-intensive. Therefore, we warn that primary schools have a higher risk than high schools in disease transmission, thereby less suitable for pushing school reopens.

Our findings also have an extensible impact on all the densely contacting communities, such as universities, military barracks, and prisons. Individuals in these environments spend much time in close contact (e.g., sitting and living in the same room) so that the virus can have sufficient time to transmit among humans. Using DCT technology to trace the possible epidemic spreading routes and quarantine the higher risk groups (e.g., direct contacts) can help prevent a pandemic in the entire community but with minimum cost, compared to a full-scale shutdown. Accordingly, we suggest that the concerned organizations with sufficient economic status resources should consider adopting DCT technology to prevent disease spreading while maintaining their regular operations.

References

[1] M. Peng, "Outbreak of COVID-19: An emerging global pandemic threat," *Biomed. Pharmacotherapy*, vol. 129, Sep. 2020, Art. no. 110499.

[2] G. Mohler *et al.*, "Impact of social distancing during COVID-19 pandemic on crime in los angeles and indianapolis," *J. Criminal Justice*, vol. 68, May 2020, Art. no. 101692.

[3] T. P. B. Thu, P. N. H. Ngoc, N. M. Hai, and L. A. Tuan, "Effect of the social distancing measures on the spread of COVID-19 in 10 highly infected countries," *Sci. Total Environ.*, vol. 742, Nov. 2020, Art. no. 140430.

[4] B. Patterson *et al.*, "A novel cohorting and isolation strategy for suspected COVID-19 cases during a pandemic," *J. Hospital Infection*, vol. 105, no. 4, pp. 632–637, Aug. 2020.

[5] Q. Cui, Z. Hu, Y. Li, J. Han, Z. Teng, and J. Qian, "Dynamic variations of the COVID-19 disease at different quarantine strategies in Wuhan and mainland China," *J. Infection Public Health*, vol. 13, no. 6, pp. 849–855, Jun. 2020.

[6] M. Chan Sun and C. B. Lan Cheong Wah, "Lessons to be learnt from the COVID-19 public health response in mauritius," *Public Health Pract.*, vol. 1, Nov. 2020, Art. no. 100023.

[7] B. D. Singer, "COVID-19 and the next influenza season," *Sci. Adv.*, vol. 6, no. 31, Jul. 2020, Art. no. eabd0086.

[8] R. E. Glover *et al.*, "A framework for identifying and mitigating the equity harms of COVID-19 policy interventions," *J. Clin. Epidemiol.*, vol. 128, pp. 35–48, Dec. 2020.

[9] N. Oliver *et al.*, "Mobile phone data for informing public health actions across the COVID-19 pandemic life cycle," *Sci. Adv.*, vol. 6, no. 23, Jun. 2020, Art. no. eabc0764.

[10] S. Yoo and S. Managi, "Global mortality benefits of COVID-19 action," *Technol. Forecasting Social Change*, vol. 160, Nov. 2020, Art. no. 120231.

[11] C. Viboud *et al.*, "Risk factors of influenza transmission in households," *Brit. J. Gen. Pract.*, vol. 54, no. 506, pp. 684–689, 2004.

[12] S. Cauchemez *et al.*, "Closure of schools during an influenza pandemic," *Lancet Infectious Diseases*, vol. 9, no. 8, pp. 473–481, Aug. 2009.

[13] V. Gemmetto, A. Barrat, and C. Cattuto, "Mitigation of infectious disease at school: Targeted class closure vs school closure," *BMC Infectious Diseases*, vol. 14, no. 1, p. 695, Dec. 2014.

[14] M. Litvinova, Q.-H. Liu, E. S. Kulikov, and M. Ajelli, "Reactive school closure weakens the network of social interactions and reduces the spread of influenza," *Proc. Nat. Acad. Sci. USA*, vol. 116, no. 27, pp. 13174–13181, 2019.

[15] S. T. Brown *et al.*, "Would school closure for the 2009 H1N1 influenza epidemic have been worth the cost?: A computational simulation of pennsylvania," *BMC Public Health*, vol. 11, no. 1, p. 353, Dec. 2011.

[16] E. Beaunoyer, S. Dupéré, and M. J. Guitton, "COVID-19 and digital inequalities: Reciprocal impacts and mitigation strategies," *Comput. Hum. Behav.*, vol. 111, Oct. 2020, Art. no. 106424.

[17] A. Vespignani *et al.*, "Modelling COVID-19," *Nature Rev. Phys.*, vol. 2, no. 6, pp. 279–281, 2020.

[18] H.-C. Sun, M.-D. Xu, and X.-K. Xu, "Infection and prevention of COVID-19 in schools based on real-life interpersonal contact data," *J. Univ. Electron. Sci. Technol. China*, vol. 49, no. 3, pp. 399–407, 2020.

[19] B. Rockx *et al.*, "Comparative pathogenesis of COVID-19, mers, and SARs in a nonhuman primate model," *Science*, vol. 368, no. 6494, pp. 1012–1015, 2020.

[20] Y. Liu *et al.*, "What are the underlying transmission patterns of COVID-19 outbreak? An age-specific social contact characterization," *EClinicalMedicine*, vol. 22, May 2020, Art. no. 100354.
[21] C. Cattuto, W. Van den Broeck, A. Barrat, V. Colizza, J.-F. Pinton, and A. Vespignani, "Dynamics of person-to-person interactions from distributed RFID sensor networks," *PLoS ONE*, vol. 5, no. 7, Jul. 2010, Art. no. e11596.
[22] R. Wang *et al.*, "StudentLife: Assessing mental health, academic performance and behavioral trends of college students using smartphones," in *Proc. ACM Int. Joint Conf. Pervas. Ubiquitous Comput.*, Sep. 2014, pp. 1–6.
[23] M. Zhou, M. Ma, Y. Zhang, K. SuiA, D. Pei, and T. Moscibroda, "EDUM: Classroom education measurements via large-scale wifi networks," in *Proc. Int. Joint Conf. Pervas. Ubiquitous Comput.* New York, NY, USA: Association for Computing Machinery, 2016, p. 316–327.
[24] Y. Cao *et al.*, "Orderliness predicts academic performance: Behavioural analysis on campus lifestyle," *J. Roy. Soc. Interface*, vol. 15, no. 146, Sep. 2018, Art. no. 20180210.
[25] H. Yao, D. Lian, Y. Cao, Y. Wu, and T. Zhou, "Predicting academic performance for college students: A campus behavior perspective," *ACM Trans. Intell. Syst. Technol.*, vol. 10, no. 3, pp. 1–21, May 2019.
[26] J. Stehlã *et al.*, "High-resolution measurements of face-to-face contact patterns in a primary school," *PLoS ONE*, vol. 6, no. 8, pp. 1–13, 2011.
[27] *The Sociopatterns Collaboration*. Accessed: Apr. 8, 2020. [Online]. Available: http://www.sociopatterns.org/.
[28] L. Ferretti *et al.*, "Quantifying dynamics of SARs-cov-2 transmission suggests that epidemic control and avoidance is feasible through instantaneous digital contact tracing," *Science*, vol. 368, no. 619, 2020, Art. no. eabb6936.
[29] C. O. Buckee *et al.*, "Aggregated mobility data could help fight COVID-19," *Science*, vol. 368, no. 6487, pp. 145–146, 2020.
[30] N. Ahmed *et al.*, "A survey of COVID-19 contact tracing apps," *IEEE Access*, vol. 8, pp. 134577–134601, 2020.
[31] E. Hernandez-Orallo, P. Manzoni, C. Calafate, and J.-C. Cano, "Evaluating how smartphone contact tracing technology can reduce the spread of infectious diseases: The case of covid-19," *IEEE Access*, vol. 8, pp. 99083–99087, 2020.
[32] A. J. Kucharski *et al.*, "Effectiveness of isolation, testing, contact tracing, and physical distancing on reducing transmission of SARS-CoV-2 in different settings: A mathematical modelling study," *Lancet Infectious Diseases*, vol. 20, no. 10, pp. 1151–1160, 2020.
[33] X. He *et al.*, "Temporal dynamics in viral shedding and transmissibility of COVID-19," *Nature Med.*, vol. 26, no. 5, pp. 1–8, 2020.
[34] B. J. Cowling *et al.*, "Comparative epidemiology of human infections with avian influenza a h7n9 and h5n1 viruses in China: A population-based study of laboratory-confirmed cases," *Lancet*, vol. 382, no. 9887, pp. 129–137, 2013.
[35] Z. Du, C. Nugent, A. P. Galvani, R. M. Krug, and L. A. Meyers, "Modeling mitigation of influenza epidemics by baloxavir," *Nature Commun.*, vol. 11, no. 1, p. 2750, Dec. 2020.
[36] W. Guan *et al.*, "Clinical characteristics of coronavirus disease 2019 in China," *New England J. Med.*, vol. 382, pp. 1708–1720, 2020.
[37] D. Wang *et al.*, "Clinical characteristics of 138 hospitalized patients with 2019 novel coronavirus-infected pneumonia in Wuhan, China," *JAMA*, vol. 323, no. 11, pp. 1061–1069, 2020.
[38] S. Zhao *et al.*, "Preliminary estimation of the basic reproduction number of novel coronavirus (2019-ncov) in China, from 2019 to 2020: A data-driven analysis in the early phase of the outbreak," *Int. J. Infectious Diseases*, vol. 92, pp. 214–217, 2020.
[39] S. Sanche, Y. T. Lin, C. Xu, E. Romero-Severson, N. Hengartner, and R. Ke, "High contagiousness and rapid spread of severe acute respiratory syndrome coronavirus 2," *Emerg. Infectious Diseases*, vol. 26, no. 7, pp. 1470–1477, Jul. 2020.
[40] D. Brockmann and D. Helbing, "The hidden geometry of complex, network-driven contagion phenomena," *Science*, vol. 342, no. 6164, pp. 1337–1342, Dec. 2013.
[41] W.-W. Sun, F. Ling, and J.-R. Pan, "Epidemiological characteristics of 2019 novel coronavirus family clustering in Zhejiang Province," *Chin. J. Preventive Med.*, vol. 54, no. 6, p. E027, 2020.
[42] M. Day, "Covid-19: Four fifths of cases are asymptomatic, China figures indicate," *BMJ*, vol. 369, p. m1375, Apr. 2020.

Hao-Chen Sun received the bachelor's degree from the School of Software and Microelectronics, Harbin University of Science and Technology, Harbin, China, in 2019. He is currently pursuing the M.S. degree with the College of Information and Communication Engineering, Dalian Minzu University, Dalian, China.

His research interests include social network analysis and disease transmission modeling.

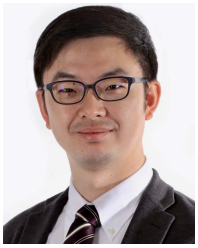

Xiao-Fan Liu (Member, IEEE) received the B.Sc. (Hons.) and Ph.D. degrees in electronic and information engineering from the Hong Kong Polytechnic University, Hong Kong, in 2008 and 2012, respectively.

He is currently an Assistant Professor with the City University of Hong Kong, Hong Kong. His research interests include cryptocurrency, blockchain, and social network analysis.

Zhan-Wei Du received the Ph.D. degree from the Department of Computer Science and Technology, Jilin University, Changchun, China, in 2015.

He is currently a Research Assistant Professor with the School of Public Health, LKS Faculty of Medicine, The University of Hong Kong, Hong Kong. His current research interests include complex networks, smart city of traffic networks, and epidemic disease propagation.

Xiao-Ke Xu (Member, IEEE) received the Ph.D. degree from the College of Information and Communication Engineering, Dalian Maritime University, Dalian, China, in 2008.

He was a Post-Doctoral Fellow with Hong Kong Polytechnic University, Hong Kong. He is currently a Professor with the College of Information and Communication Engineering, Dalian Minzu University. His current research interests are in community detection and data mining on social networks.

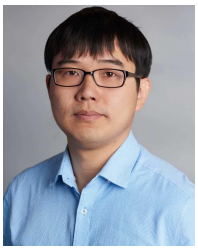

Ye Wu received the Ph.D. degree from the University of Potsdam, Potsdam, Germany.

He is currently a Professor with the School of Journalism and Communication, Beijing Normal University, Beijing, China. His current research interests are in computational communication and information spreading.